Diesel Engine Performance, Emissions and Combustion Characteristics of Biodiesel and Its Blends Derived from Catalytic Pyrolysis of Waste Cooking Oil

Mohamed Mohamed [1,2,*] , **Chee-Keong Tan [1]**, **Ali Fouda [3]**, **Mohammed Saber Gad [4]**,
Osayed Abu-Elyazeed [5] and **Abdel-Fatah Hashem [2]**

[1] School of Engineering, University of South Wales, Pontypridd CF23 1DL, UK; ck.tan@southwales.ac.uk
[2] Department of Mechanical Engineering, Faculty of Engineering, South Valley University, Qena 83523, Egypt; fatah_hashem@yahoo.com
[3] Department of Mechanical Power Engineering, Faculty of Engineering, Mansoura University, Mansoura 35516, Egypt; eng.alifouda.2007@yahoo.com
[4] Mechanical Engineering Department, Faculty of Engineering, Fayoum University, Fayoum 63514, Egypt; mgad27@yahoo.com
[5] Department of Mechanical Engineering, Faculty of Engineering, Helwan University, Mataria 11795, Egypt; bio_new_life@hotmail.com
* Correspondence: mohamed.mohamed@southwales.ac.uk

Abstract: This paper first describes a slow catalytic pyrolysis process used for synthesizing biodiesel from waste cooking oil (WCO) as a feedstock. The influence of variations in the catalyst type (sodium hydroxide and potassium hydroxide), and catalyst concentration (0.5, 1.0, 3.0, 5.0, 7.0 and 10.0% by weight) on both the pyrolysis temperature range and biodiesel yield were investigated. The results suggested that sodium hydroxide (NaOH) was more effective than potassium hydroxide (KOH) as catalysts and that the highest yield (around 70 wt.%) was observed for a NaOH concentration of about 1 wt.% The resultant pyrolysis temperature range was also significantly lower for NaOH catalyst, thus suggesting overall lower energy consumption. Compared to conventional diesel, the synthesized biodiesel exhibited relatively similar physical properties and calorific value. The biodiesel was subsequently blended with diesel fuel in different blend ratios of 0, 20, 40, 60, 80 and 100% by volume of biodiesel and were later tested in a compression ignition engine. Brake thermal efficiency and specific fuel consumption were observed to be worse with biodiesel fuel blends particularly at higher engine load above 50%. However, NOx emission generally decreased with increasing blend ratio across all engine load, with greater reduction observed at higher engine load. Similar observation can also be concluded for CO emission. In contrast, lower hydrocarbon (HC) emission from the biodiesel fuel blends was only observed for blend ratios no higher than 40%. Particulate emission from the biodiesel fuel blends did not pose an issue given its comparable smoke opacity to diesel observed during the engine test. The in-cylinder peak pressures, temperature and heat release rate of biodiesel fuel blends were lower than diesel. Overall, biodiesel fuel blends exhibited shorter ignition delays when compared to diesel fuel.

Keywords: biodiesel; waste cooking oil (WCO); pyrolysis; emissions; combustion characteristics

1. Introduction

The continual depletion in the world of fossil fuel resources along with the increasing demand in energy consumption has prompted the need for the production and utilisation of alternative fuels. Among other alternative fuels, biodiesel has received considerable attention worldwide [1]

due to a number of advantages, such as, being renewable, a potential for waste sources recycling, its simplicity and flexibility in the production methods, and its reduced emissions when compared to conventional diesel [2]. Although a wide variety of feedstock could be used to produce biodiesel, by far the most utilised resources on a large industrial scale are still attributed to high-quality edible oils [3]. This has been largely due to the security in the supply chain and their lower content in Free Fatty Acid (FFA). There have been numerous hot debates about the sustainability of the current approaches to the feedstock supply chain, especially given their potentially negative impact on the global food security in the long term. Consequently, a growing number of studies to test the viability of different alternative feedstock materials have been reported in the literature. These included, but were not limited to, non-edible oil-bearing plants, such as Jatropha Curcas, Soapnut, Castor beans [4–6], as well as non-edible waste fat from animal carcasses [7].

Transesterification remained the most popular chemical reaction process for converting raw oil/fat (triglyceride) into biodiesel (fatty acid methyl-ester; FAME) at industrial scale. Nowadays, most of the commercially produced biodiesel uses alkali-catalysed transesterification for economical reason, due to its relatively fast reaction rate and low temperatures and pressure required [8]. However, when dealing with feedstock containing a high percentage of FFA, a pre-treatment process (esterification) used to convert the excessive FFA to methyl ester is required, thereby increasing overall processing cost. This step is crucial as, without it, there is tendency of forming larger amounts of long-chain saturated FAME (which results in poor low-temperature properties of the biodiesel produced), and reduced biodiesel yield [9]. Recent advances to further intensify the transesterification process have also been reported [10,11], which ranged from the use of non-catalytic supercritical alcohol, microwave and ultrasound assisted transesterification, to more sophisticated plasma reactor technology. However, issues associated with equipment cost, energy consumption and scale-up still present some challenges.

On the other hand, the pyrolysis of oils and animal fat has also been investigated [6,9,12], where materials are thermally decomposed (with or without catalyst) at elevated temperature in the absence of oxygen to produce biodiesel suitable for diesel engine. Proven commercial technology for pyrolysis of solid biomass and waste materials to produce bio-oil has been around for many years. This technology may provide a promising alternative to transesterification due to feedstock flexibility and adaptability to existing infrastructure [13]. This is also believed to be the driver behind the growing amount of research recently in co-pyrolysis of waste oil with solid biomass and other waste materials [14–16]. Compared to transesterification, a number of studies have shown that bio-oil produced via pyrolysis processes may possess better properties, such as lower viscosity, lower freezing point and higher cetane number [17,18]. In addition, the compositions of the biofuel produced can be tuned by altering the operating conditions so that this allows for a process able to tailor the products towards certain applications [19].

The impact of biodiesel fuel blends on the performances and emissions of diesel engines has been the subject of extensive research for a number of years, as summarised in [20,21]. Obviously, almost all of the reported case studies involved biodiesel produced from transesterification processes for the reason of popularity, mentioned above. Engine tests with higher blend ratios up to 100% pure biodiesel are also very limited. Nonetheless, these studies concluded that biodiesel derived from a wide range of feedstock can be used in conventional diesel engine (up to 20% blend ratio) with little or no modification. Although these authors also attempted to provide a general view on engine performances and emissions, it was obviously difficult to draw specific conclusions due to large variability in the feedstock materials, additive used, engine types and operating parameters. From the literature review conducted so far, there appears to be limited work carried out on engine testing of biodiesel produced from the pyrolysis of waste cooking oil, and that is the subject of study in this paper. The use of waste cooking oils as sustainable feedstock for biodiesel production makes sense, since it is both economically and environmentally friendly.

Therefore, the aim of this paper is to investigate the impact of biodiesel and its blends, produced from catalytic pyrolysis of waste cooking oil, on the performances of a laboratory scale

compression ignition engine. In the current work, waste-cooking oil (WCO) collected from different restaurants were first blended and filtered to remove all the solid residual. A laboratory-scale pyrolysis rig was then used to process the WCO to produce the biodiesel. The influence of the catalyst type and its concentrations on the pyrolysis temperature range and biodiesel yield were then investigated. The biodiesel was subsequently tested in a laboratory-scale diesel engine, covering blend ratios up to 100% pure biodiesel (B100). The engine performances, emissions and combustion characteristics for biodiesel blends were compared with crude diesel to obtain the optimum blending.

Biodiesel Production from Pyrolysis of Waste Cooking Oil

Figure 1 shows the schematic diagram of the test facilities used for pyrolysis of the waste-cooking oil (WCO). This same test facility has also been used successfully in two previous published works [6,22]. Detailed dimension of the oil tank is shown in Figure 2, which was designed and manufactured from stainless steel for withstanding the corrosive and high temperature environment. The tank has a circular base of 190 mm diameter and 265 mm in height for a holding capacity of up to 5 L of WCO. The tank was well insulated to minimize heat losses to the surrounding. A circular electric heater of 1400 watt was attached to the oil tank to heat up the WCO. For each test, 1.5 L of WCO was used and the biodiesel vapour generated from the reactor tank was condensed in a condenser constructed from 29 mm (bore) × 800 mm (length) of high-quality borosilicate glass tube and subsequently collected in a two litre PYREX flask. Excess moisture from the biodiesel was removed by further heating to 100 °C under atmospheric conditions. The high viscosity black residuals from the pyrolyzed WCO precipitate on the bottom of the reactor, which is known as bio-mazut. During the experiments, a K-type thermocouple (±1% accuracy) was installed on the top of the tank to monitor the biodiesel vapour temperature, which serves as an indication of the pyrolysis temperature.
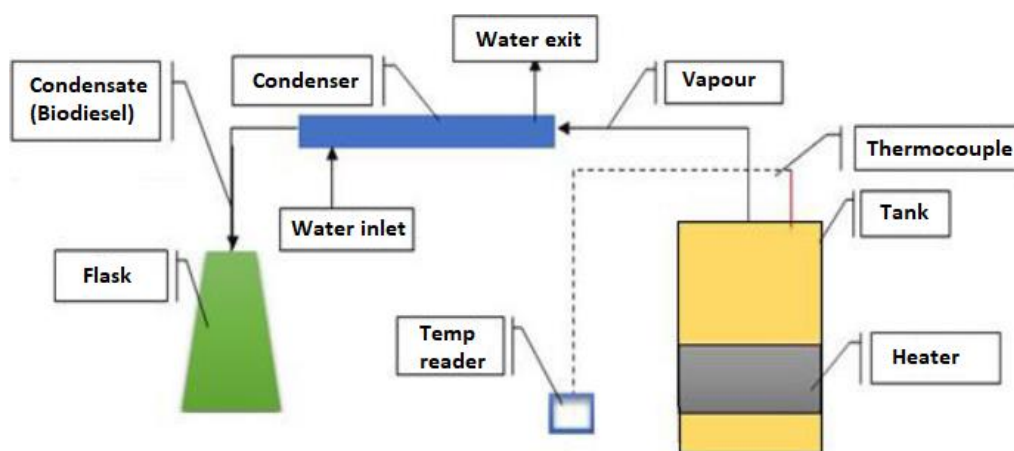
Figure 1. Schematic diagram for the test rig used in pyrolysis process of WCO (Adapted from [23]).

Similar to the investigation conducted in [6] for raw castor oil, both sodium hydroxide (NaOH) and potassium hydroxide (KOH) were used as catalyst for the pyrolysis reaction. A series of tests were first conducted, using NaOH as the catalyst, to show the effect of the catalyst concentration on biodiesel yield, as shown in Figure 3a. It was found that the present of 1% NaOH resulted in the highest biodiesel yield, which is consistent with the previous finding on raw castor oil. However, using WCO as feedstock provided lower yield (70 wt.%) than that of raw castor oil (92 wt.%). Using 1% catalyst concentration as the benchmark, a further comparison of the effectiveness of NaOH and KOH as catalyst is shown in Figure 3b, from which it can be concluded that KOH is much less effective in the current study. This may be partly because the average pyrolysis temperature was lower when using NaOH as catalyst as indicated in Figure 3c, which resulted in lower rate of formation of solid tar residual. The lower pyrolysis temperature range also implied lower overall energy consumption. It is interesting that a different investigation [24] of biodiesel production from used cooking oil via

transesterification also indicated that NaOH catalyst delivers the most favourable option in terms of energy consumption. However, because of the higher temperature involved in pyrolysis, the cost of energy consumption will be higher than that of the transesterification process. Figure 3d shows a sample of the filtered WCO before the pyrolysis process (left) and the final biodiesel produced (right).
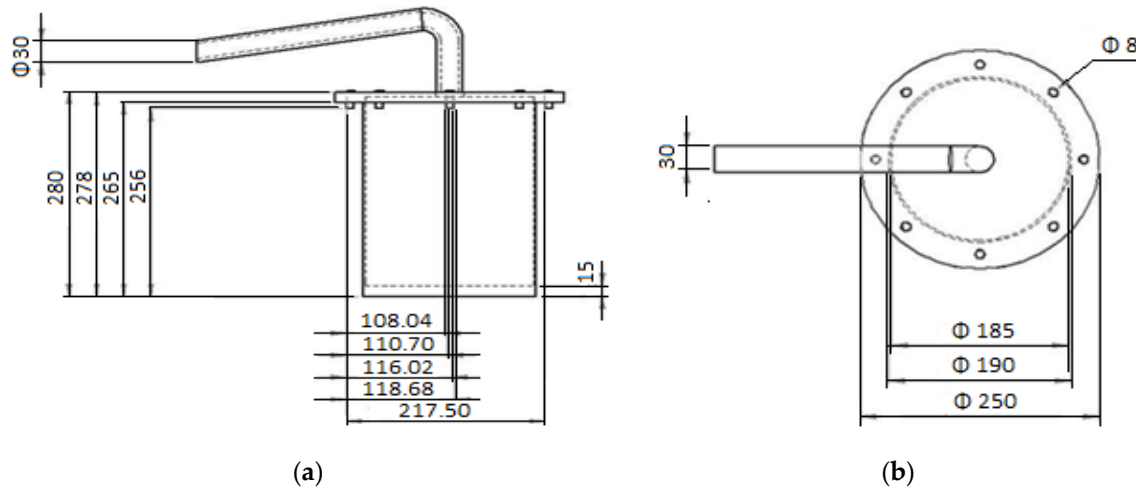

(**a**)   (**b**)

Figure 2. Cylindrical oil tank with dimensions in mm, (**a**) front view and (**b**) plan view (Adapted from [23]).

(**a**)   (**b**)
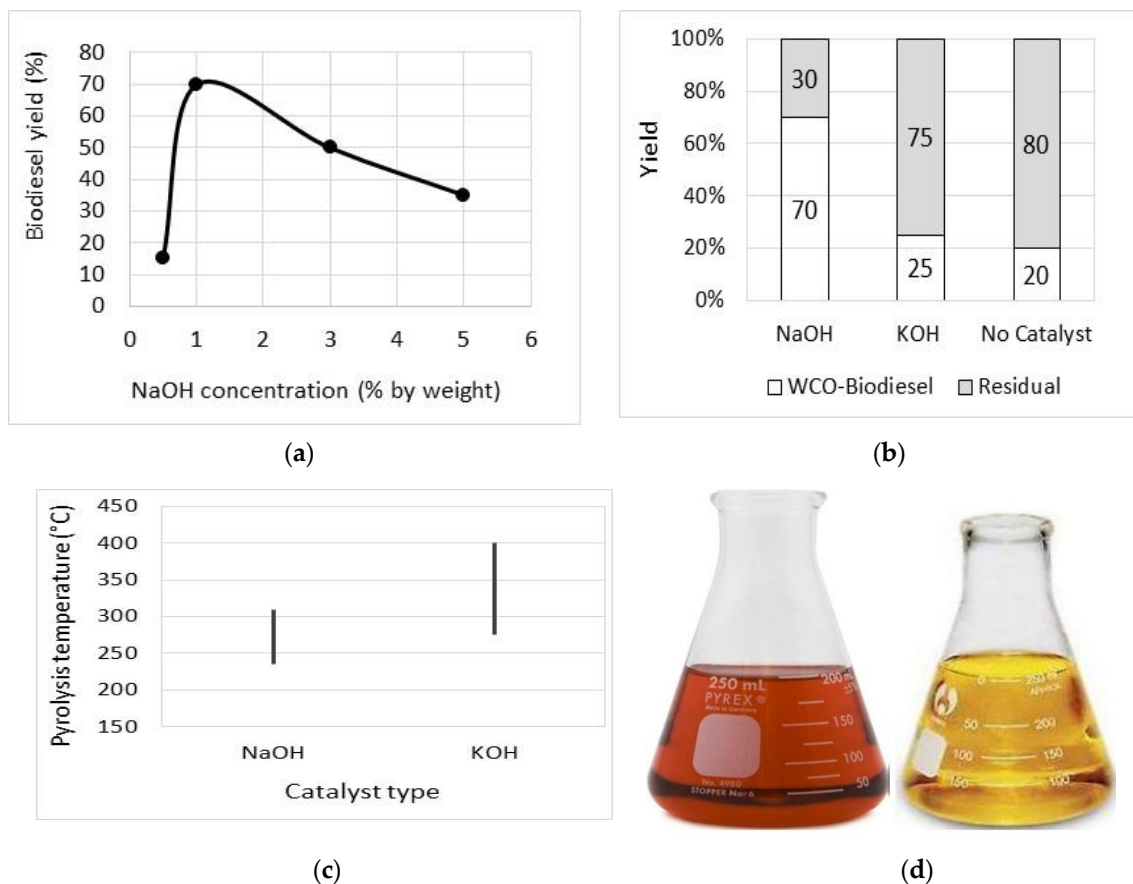

(**c**)   (**d**)

Figure 3. (**a**) Effect of NaOH concentrations on biodiesel yield, (**b**) Effect of NaOH and KOH (1 wt.% concentration) as catalyst for the pyrolysis of WCO, (**c**) Pyrolysis temperature range, and (**d**) Physical appearance of WCO and biodiesel.

Table 1 shows the physical properties of diesel and synthesized biodiesel used for the engine test. The density, higher heating value, and corrosiveness of the biodiesel are similar to diesel fuel. Particularly, similar density (2.3% difference) should lead to complete physical mixing between the biodiesel and diesel without separation. The lower density and viscosity of the biodiesel should also give rise to more effective fuel-atomization. The lower pour point of the biodiesel would also facilitate the start-up and operation of engines in cold climate. Furthermore, negligible sulphur content in the biodiesel would reduce emissions of hydrocarbons and oxides of nitrogen (precursors of ozone), as well as particulate matter. Due to the nature of the pyrolysis process, the biodiesel contains higher carbon residual as a result from formation of longer-chain hydrocarbon. Nonetheless, the increase in the aromatic and unsaturated hydrocarbon from the pyrolysis process also led to a slight increase in the calorific value of the biodiesel.

Table 1. Physical properties of both traditional diesel and biodiesel.

Property	Unit	Diesel (as-Received)	Diesel Standards	B100	Standard ASTM Method
Density at 15 °C	kg/m^3	835.8	832.0	816.6	D4052
Colour	-	2	0.85	6	D6045
Kinematic Viscosity at 40 °C	cSt	4.95	1.0–6.7	2.288	D7042
Pensky Flashpoint Closed cup	°C	Minimum 55	Minimum 55	28	D93
Pour point	°C	−9	3–15	−27	D6749
Sulphur Content	wt.%	1.5	Maximum 1	nil	D4294
Ash	% vol.	nil	Maximum 0.01	0.00312	D482
Carbon Residue	wt.%	0.1	Maximum 0.1	1.031	D4530
Cetane Number	-	51.86	Minimum 46	54.6	D4737
Cu-strip corrosion at 50 °C for 3 h	-	Maximum 1	Maximum 1	1	D130
Calorific value	MJ/kg	45.62	Minimum 44.3	46.62	D4868

2. Experimental Setup for Engine Tests

The biodiesel and its blends were subsequently tested in a single cylinder, four strokes, air-cooled, direct injection diesel engine. The engine speed was measured using a speed tachometer. The schematic diagram of the engine test bed is shown in Figure 4 and the technical specifications of the engine are listed in Table 2. The Direct Current (DC) generator was equipped with a load controller (maximum electrical power output of 10.5 kW) and was coupled directly to the engine to measure the brake power. The intake airflow rate was calculated from measuring the pressure drop (via a differential manometer) across a sharp-edged orifice before flowing into the engine. Calibrated K-type thermocouples were used for temperature measurements at different locations on the engine, which includes the intake air and exhaust manifolds. At the beginning of each test, the engine was run for approximately 20 min to reach a steady state before measurements commenced. Subsequently, a fixed amount of fuel (30 cm^3) was consumed for each recording period, which then allowed for the average fuel flow rate to be determined. The injection pressure of the fuel was set by adjusting the spring tension of the fuel injector. The instantaneous in-cylinder pressure was measured by a water cooled Kistler piezoelectric pressure transducer (model 601A) coupled with a Nexus charge amplifier (2692-A-0S4). The piezoelectric pressure transducer was flush mounted with the cylinder head to measure the combustion pressure. Flush mounting was preferred to minimize the lag in the pressure signal and to avoid resonance caused by the connecting pipe. The instantaneous position of the piston Top Dead Centre (TDC) was determined using a proximity switch (Type LM12-3004PA), which was fixed on the output shaft of the engine. The combustion pressure data were averaged over 120 consecutive engine cycles. LABVIEW software and national instruments data acquisition card (NI-USB-6210) were used for data acquisition.

An OPA 100 smoke meter and MRU DELTA 1600-V gas analyser were used for smoke opacity and exhaust gas emissions concentrations measurements, respectively. The experiment was carried out by varying load from 20% to 100% while maintaining at constant engine speed of 1500 rpm. The overall uncertainty of the experiment was calculated by the following equation by summing the uncertainties in each individual variable (see Table 3):

$$
\begin{aligned}
w_R &= \left[\begin{array}{c} (uT_{exh})^2 + \left(u_{bp}\right)^2 + \left(u_{sfc}\right)^2 + (uN)^2 + (u\eta_b)^2 + (uCO)^2 + (uHC)^2 \\ + (uNO_x)^2 + \left(uP_{cyl}\right)^2 + (uTDC)^2 \end{array} \right]^{1/2} \\
&= \left[\begin{array}{c} (0.75\%)^2 + (0.85\%)^2 + (2.20\%)^2 + (0.15\%)^2 + (1.50\%)^2 + (0.01\%)^2 + (1.00\%)^2 \\ + (1.00\%)^2 + (0.20\%)^2 + (1.00\%)^2 \end{array} \right]^{1/2} \\
&= 3.38\%
\end{aligned}
$$

where:

uT_{exh}: Uncertainty of exhaust gas temperature.

u_{bp}: Uncertainty of brake power.

u_{sfc}: Uncertainty of specific fuel consumption.

uN: Uncertainty of engine speed.

$u\eta_b$: Uncertainty of brake thermal efficiency.

uCO: Uncertainty of CO emission.

uHC: Uncertainty of HC emission.

uNO_x: Uncertainty of NOx emission.

uP_{cyl}: Uncertainty of cylinder pressure transducer.
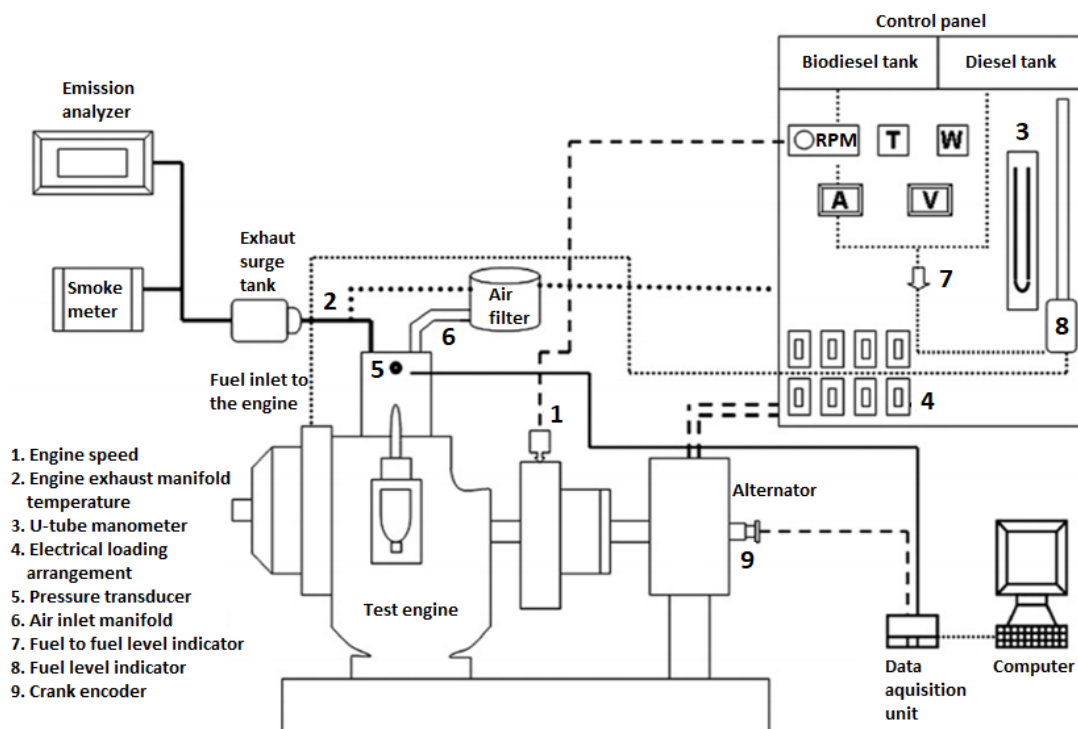
$uTDC$: Uncertainty of TDC proximity switch.

Figure 4. Schematic diagram of a diesel test engine.

Table 2. Engine specifications.

Model	DEUTZ (FI L511)
Number of cylinders	1
Number of cycles	4
Bore, mm	100
Stroke, mm	105
Displacement, c.c	825
Connecting rod length, mm	180
Compression ratio	17:1
Idle speed, rpm	900
Rated speed, rpm	1500
Max. engine load, kW	5.775
Fuel injection timing	24° Before TDC
Injection pressure, bar	175
Type of injection	Direct injection

Table 3. Uncertainty of measuring instruments.

Variable	Uncertainty
Engine speed	±0.15%
Cylinder pressure	±0.20%
Position of TDC	±1.00%
Exhaust gas temperature	±0.75%
Exhaust gas analyser	NO: ±1.00%
	HC: ±1.00%
	CO: ±0.01%
Brake power	±0.85%
Brake thermal efficiency	±1.50%
Specific fuel consumption	±2.20%

3. Results and Discussion

3.1. Engine Performance and Emissions Characteristics

Figure 5a,b shows how the brake thermal efficiency (BTHE) and specific fuel consumption (BSFC) vary with engine loads and biodiesel blend ratios at fixed engine speed of 1500 rpm. In general, regardless of blend ratio, the BTHE increases with engine load initially before dropping off again towards full load. The optimum engine load occurred at around 75% of full load. This behaviour is consistent with the inverse trend for the BSFC. It is worth mentioning that previous study on the same engine test bed [25], using biodiesel produced from transesterification of waste cooking, delivered an optimum engine load at about 52% of full load. Therefore, the current study seems to suggest that, with biodiesel produced from pyrolysis process, the engine could be run closer to its full capacity without adversely jeopardising its efficiency and fuel consumption. Nonetheless, it is clear that conventional diesel still delivered better engine performance overall across the full range of engine load. The negative impact of higher blend ratios (above B40) can also be observed to be worse at higher engine load above 50%. Since the injector geometry and pressure remained the same

throughout the tests, these variations in the engine performance were likely due to the differences in the actual thermo-physical properties between the diesel fuel and biodiesel fuel blends.


(**a**)
(**b**)
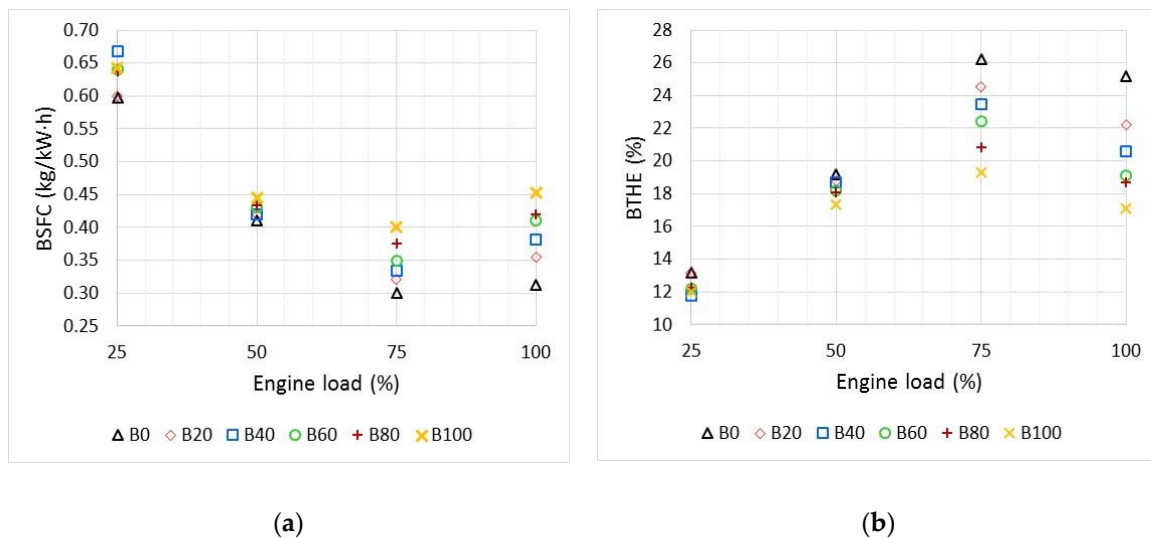
Figure 5. Influence of biodiesel blend ratio and engine load on (**a**) brake specific fuel consumption (BSFC) and (**b**) brake thermal efficiency (BTE).

In contrast to other studies [25–28] on waste-cooking oil derived biodiesel (mainly from transesterification), the calorific value of biodiesel obtained from slow pyrolysis process in the current study was higher than the tested diesel fuel. In this case the difference was about 2% higher as noted in Table 1, as opposed to 9–21% lower in the cited studies mentioned above, so that it would not be thought to considerably affect the engine performance. Nevertheless, this indicated that pyrolysis might be the better processing option to produce biodiesel with a comparable calorific value of a conventional diesel. Secondly, the viscosity of the current biodiesel was about 53% lower, whereas in the cited studies above, the viscosity of the biodiesel was between 44–96% higher than the tested diesel fuel. Therefore, it can be argued that, in the current study, viscosity would play a bigger role in influencing the engine performance. While the lower viscosity of the biodiesel fuel blends may have improved atomization and vaporisation characteristics, the resultant spray cone angle (an important parameter for spray characterisation) can become excessively wide, which can lead to negative impact on the fuel-air mixing and hence the combustion behaviour in the engine as suggested in [29]. Therefore, it can be reasonably argued that the latter may have led to a less than optimum spray penetration. This was believed to have caused an increase in the specific fuel consumption and hence reduction in efficiency of the engine. Nevertheless, it is anticipated that, with proper tuning of the injector geometry and pressure, the issue with spray angle can be practically resolved.

3.2. Engine Emissions Characteristics

In terms of emission characteristics, it can be observed from Figure 6a that, regardless of the blend ratios, NOx emission increases with the engine load in general. Interestingly, increasing the blend ratio was found to better suppress high NOx formation at higher engine load, noticeably beyond 25% full load. The overall lower NOx formation with increasing blend ratio is in agreement with other studies [30,31] and can be explained by the higher cetane number of the biodiesel which lead to shorter ignition delays, thus allowing longer time for subsequent combustion process to complete more uniformly.

(**a**)

(**b**)

(**c**)

(**d**)
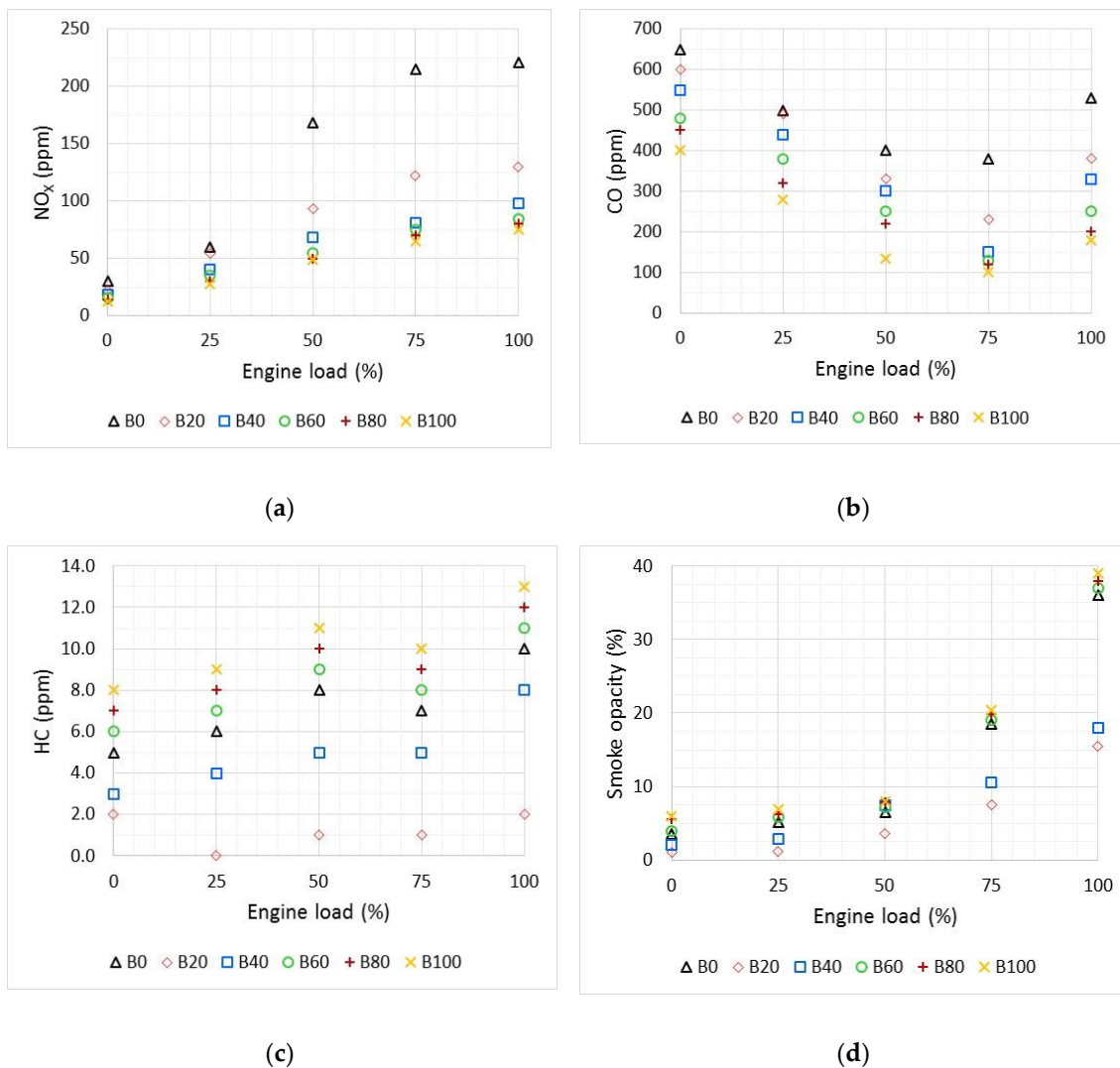
Figure 6. Influence of biodiesel blend ratio and engine load on (**a**) NOx, (**b**) CO, (**c**) hydrocarbon (HC) and (**d**) smoke opacity emissions.

For the entire engine load regime, CO emission was lower with increasing blend ratios, as shown in Figure 6b. These findings are consistent with the majority of previous studies reported in [21,32]. It is interesting to observe from Figure 6c that the reduction in the hydrocarbon (HC) emission (an important measure of combustion efficiency) was noticeable only at lower blend ratios. For higher blend ratios, B60, B80 and B100, HC emissions were higher which led to increase in the fuel consumption. This is in complete opposite trend (at least partially) as observed in a previous study on the same engine fuelled with biodiesel derived from the transesterification process [25]. The various studies reviewed in [30] also seemed to support the latter for biodiesel derived from transesterification as opposed to the pyrolysis process used in the current study. The higher oxygen content, together with the lower viscosity of the biodiesel which enhances fuel atomization and vaporization, also led to an overall lower CO emission. Blending with the biodiesel did not seem to adversely impact on particulate emission, as indicated by the observed smoke opacity in Figure 6d. If anything, reduction in the particulate matters may be accomplished by blending a small amount of the biodiesel, particularly at higher engine load.

3.3. Engine Combustion Characteristics

The cylinder pressure with respect to crank angle for all tested fuel blends at full load is illustrated in Figure 7. In general, lower peak pressures were attained when using biodiesel and this decreases consistently with increasing blend ratio. This trend is also in tandem with the lower heat release rate observed during the test as illustrated in Figure 8. As mentioned earlier in Section 3.1, the current biodiesel has a much lower viscosity than those (produced from transesterification processes) previously studied. Similar conclusions were also reported elsewhere [33,34] for biofuels produced from pyrolysis processes. This was believed to be due to the lower viscosity of the biodiesel in comparison to diesel fuel which increases the spray angle. As the result of increasing blend ratios, this progressively led to poorer fuel penetration and hence fuel-air mixing, leading to slower combustion and heat release rate.
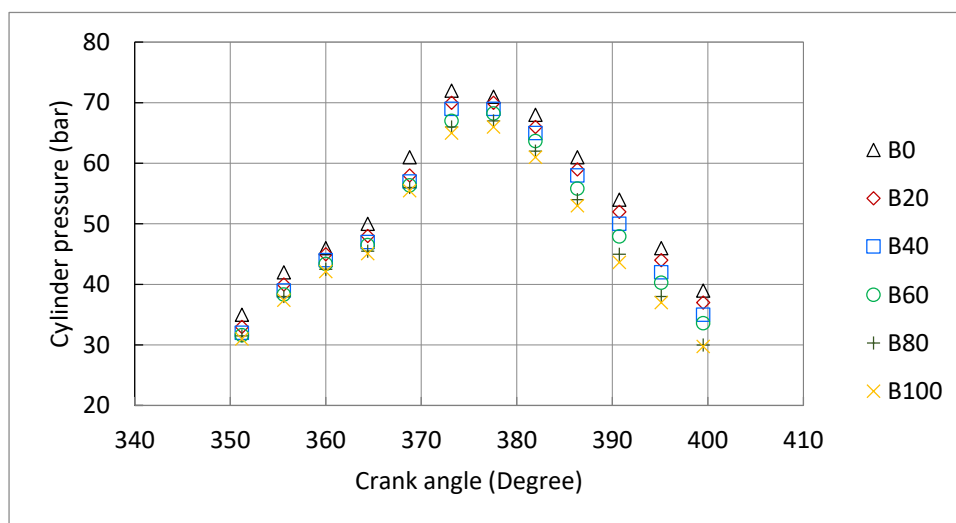
Figure 7. Effect of biodiesel blends on cylinder pressure at full load and rated speed.
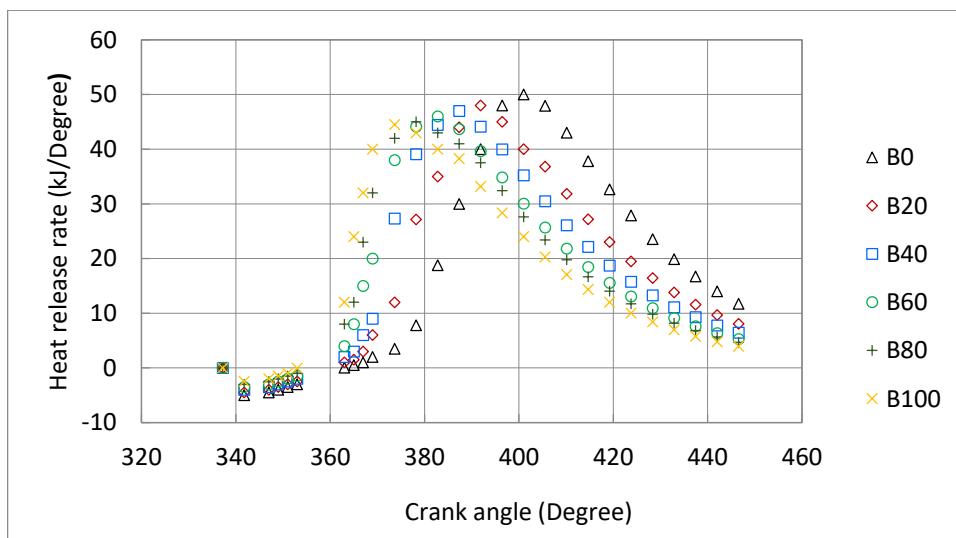

Figure 8. Heat release rate values for biodiesel blends at different crank angles and full load.

Figure 9 also indicates that the ignition delay experienced on biodiesel blends was shorter than that of 100% diesel due to the relatively higher cetane number of the biodiesel as shown in Table 1. The shorter ignition delay, together with the perceived less than optimum spray penetration also leads to lower gas temperature in the cylinder as the biodiesel blend ratios increases. Furthermore, in-cylinder gas temperature for biodiesel blends, as shown in Figure 10 at full load for illustration

purpose, was generally lower which is supported by other experimental and numerical studies reported in [35]. The overall lower in-cylinder gas temperature also explains the lower NOx emission from biodiesel observed in Figure 6 earlier. In contrast, increase in the accumulated fuel in premixed stage during the longer ignition delay period also explains the higher peak heat release rate in the case of diesel, which resulted in the overall higher in-cylinder temperature and hence NOx emission. Similar conclusions were also reported elsewhere [28,36].
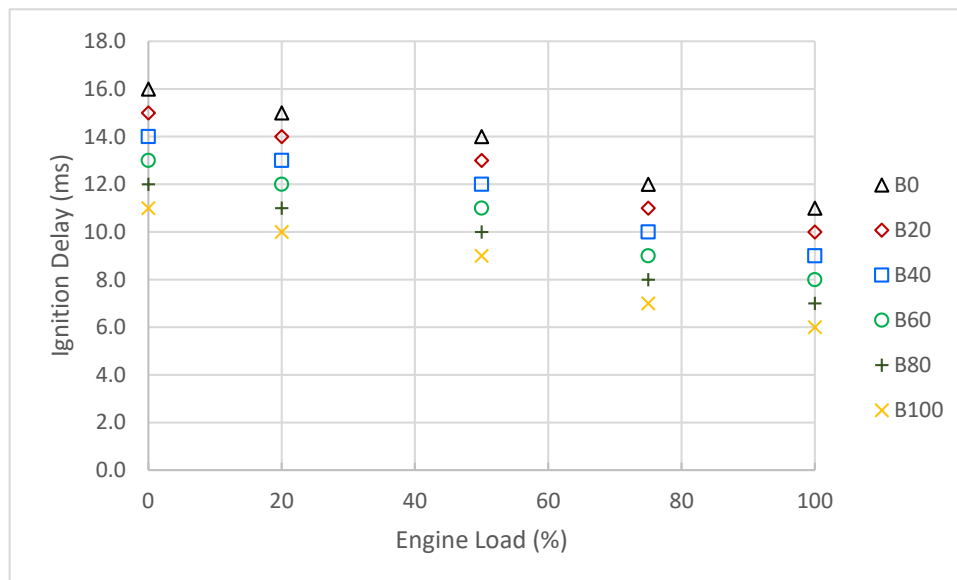
Figure 9. Ignition delay of biodiesel blends at different engine loads.
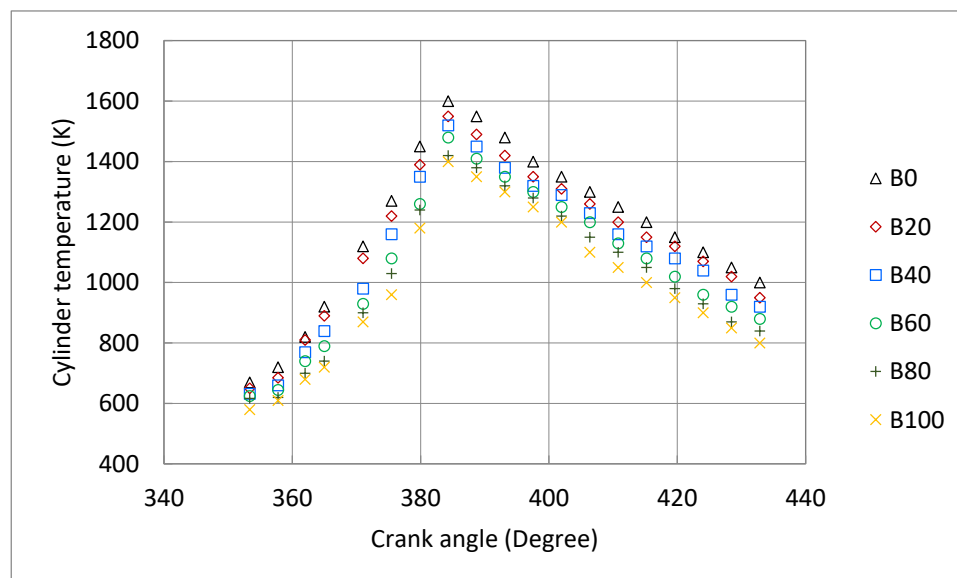
Figure 10. Cylinder temperature for biodiesel blends at different crank angles and full load.

4. Conclusions

The current study has certainly highlighted some very interesting results obtained from diesel engine test fuelled with biodiesel derived from waste-cooking oil through slow pyrolysis as opposed to transesterification process reported by the majority of previous investigations. It was found that sodium hydroxide is more effective than potassium hydroxide when used as catalyst in the pyrolysis process. Although the pyrolysis process may not match the higher yield obtained from commercially

proven transesterification processes, the biodiesel produced this way can result in higher calorific value and lower viscosity. Although the lower viscosity of the biodiesel may give rise to engine performance issues related to spray characteristics, these issues can be easily resolved by properly tuning the injector geometry and pressure. Furthermore, with the appropriate blend ratios and engine load, the current study indicated that more than 50% NOx reduction can be achieved without significantly affecting the combustion efficiency of the engine. The negative impact of higher blend ratios (above B40) on thermal efficiency was observed to be worse at a higher engine load of above 50%. CO and HC emissions were lower with increasing blend ratios. Furthermore, the higher cetane number of the biodiesel resulted in shorter ignition delay of biodiesel fuel blends, whereas the in-cylinder peak pressure, temperature and heat release rate were lower as the biodiesel blend ratio increases progressively.

References

1. Avinash, A.; Subramaniam, D.; Murugesan, A. Bio-diesel—A global scenario. *Renew. Sustain. Energy Rev.* **2014**, *29*, 517–527. [CrossRef]

2. Lin, L.; Zhou, C.S.; Vittayapadung , S.; Shen, X.; Dong, M. Opportunities and challenges for biodiesel fuel. *Appl. Energy* **2011**, *88*, 1020–1031. [CrossRef]

3. Gebremariam, S.N.; Marchetti, J.M. Economics of biodiesel production: Review. *Energy Convers. Manag.* **2018**, *168*, 74–84. [CrossRef]

4. Theogene, N.; Ikwaba, P.D. The economic feasibility of Jatropha cultivation for biodiesel production in Rwanda: A case study of Kirehe district. *Energy Sustain. Dev.* **2019**, *50*, 27–37.

5. Chen, Y.H.; Chiang, T.H.; Chen, J.H. Properties of soapnut (Sapindus mukorossi) oil biodiesel and its blends with diesel. *Biomass Bioenergy* **2013**, *52*, 15–21. [CrossRef]

6. Abdelfattah, M.S.H.; Abu-Elyazeed, O.S.M.; Abdelazeem, M.A. On biodiesels from castor raw oil using catalytic pyrolysis. *Energy* **2018**, *143*, 950–960. [CrossRef]

7. Alajmi, F.S.M.D.A.; Hairuddin, A.A.; Adam, N.M.; Abdullah, L.C. Recent trends in biodiesel production from commonly used animal fats. *Int. J. Energy Res.* **2018**, *42*, 885–902. [CrossRef]

8. Fukuda, H.; Kondo, A.; Noda, H. Biodiesel fuel production by transesterification of oils. *J. Biosci. Bioeng.* **2001**, *92*, 405–416. [CrossRef]

9. Takuya, I.; Yusuke, S.; Yusuke, K.; Motoyuki, S.; Katsumi, H. Biodiesel production from waste animal fats using pyrolysis method. *Fuel Process. Technol.* **2012**, *94*, 47–52.

10. Buchori, L.; Istadi, I.; Purwanto, P. Advanced chemical reactor technologies for biodiesel production from vegetable oils—A review. *Bull. Chem. React. Eng. Catal.* **2016**, *11*, 406–430. [CrossRef]

11. Radwan, M.S.; Ismail, M.A.; El-Feky, S.M.S.; Abu-Elyazeed, O.S.M. Jojoba Methyl Ester as a Diesel Fuel Substitute: Preparation and Characterization. *Appl. Therm. Eng.* **2017**, *21*, 314–322. [CrossRef]

12. Lappi, H.; Alén, R. Pyrolysis of vegetable oil soaps—Palm, olive, rapeseed and castor oils. *J. Anal. Appl. Pyrolysis* **2011**, *91*, 154–158. [CrossRef]

13. Aïda, B.H.T.; Kaouther, Z.; Withek, B.; Slim, N.; Aymen, O. Second generation biofuels production from waste cooking oil via pyrolysis process. *Renew. Energy* **2018**, *126*, 888–896.

14. Phetyim, N.; Pivsa-Art, S. Prototype co-pyrolysis of used lubricant oil and mixed plasticwaste to produce a diesel-like fuel. *Energies* **2018**, *11*, 2973. [CrossRef]

15. Wang, Y.P.; Dai, L.L.; Fan, L.L.; Cao, L.P.; Zhou, Y.; Zhao, Y.F.; Liu, Y.H.; Ruan, R. Catalytic co-pyrolysis of waste vegetable oil and high density polyethylene for hydrocarbon fuel production. *Waste Manag.* **2017**, *61*, 276–282. [CrossRef]

16. Chen, G.Y.; Liu, C.; Ma, W.C.; Zhang, X.X.; Li, Y.B.; Yan, B.B.; Zhou, W.H. Co-pyrolysis of corn cob and waste cooking oil in a fixed bed. *Bioresour. Technol.* **2014**, *166*, 500–507. [CrossRef]

17. Faisal Abnisa, F.; Arami-Niya, A.; Wan Daud, W.M.A.; Sahu, J.N. Characterization of bio-oil and bio-char from pyrolysis of palm oil wastes. *Bioenergy Res.* **2013**, *6*, 830–840. [CrossRef]

18. Wang, W.C.; Thapaliya, N.; Campos, A.; Stikeleather, L.F.; Roberts, W.L. Hydrocarbon fuels from vegetable oils via hydrolysis and thermo-catalytic decarboxylation. *Fuel* **2012**, *95*, 622–629. [CrossRef]

19. Wiggers, V.R.; Zonta, G.R.; França, A.P.; Scharf, D.R.; Simionatto, E.L.; Ender, L.; Meier, H.F. Challenges associated with choosing operational conditions for triglyceride thermal cracking aiming to improve biofuel quality. *Fuel* **2013**, *107*, 601–608. [CrossRef]

20. Tamilselvan, P.; Nallusamy, N.; Rajkumar, S. A comprehensive review on performance, combustion and emission characteristics of biodiesel fuelled diesel engines. *Renew. Sustain. Energy Rev.* **2017**, *79*, 1134–1159. [CrossRef]

21. Suresh, M.; Jawahar, C.P.; Richard, A. A review on biodiesel production, combustion, performance, and emission characteristics of non-edible oils in variable compression ratio diesel engine using biodiesel and its blends. *Renew. Sustain. Energy Rev.* **2018**, *92*, 38–49. [CrossRef]

22. Abu-Elyazeed, O.S.M. On the ignition delay of two types of Castor oil bio-diesel using shock tube experiments. *Fuel* **2015**, *144*, 157–163. [CrossRef]

23. Mohamed, M.A.; Hashim, A.M.; Abu-Elyazeed, O.S.; Elsayied, H.A. Biofuel production from used cooking oil using pyrolysis process. *Int. J. Res. Appl. Sci. Eng. Technol.* **2017**, *5*, 12. [CrossRef]

24. Mendecka, B.; Lombardi, L.; Kozioł, J. Probabilistic multi-criteria analysis for evaluation of biodiesel production technologies from used cooking oil. *Renew. Energy* **2020**, *147*, 2542–2553. [CrossRef]

25. Abed, K.A.; El-Morsi, A.K.; Sayed, M.M.; El-Shaib, A.A.; Gad, M.S. Effect of waste cooking-oil biodiesel on performance and exhaust emissions of a diesel engine. *Egypt. J. Petroleum.* **2018**, *27*, 985–989. [CrossRef]

26. Hirkude, J.B.; Padalkar, A.S. Performance and emission analysis of a compression ignition Engine operated on waste fried oil methyl esters. *Appl. Energy* **2012**, *90*, 68–72. [CrossRef]

27. Muralidharan, K.; Vasudevan, D.; Sheeba, K.N. Performance, emission and combustion characteristics of biodiesel fuelled variable compression ratio engine. *Energy* **2011**, *36*, 5385–5393. [CrossRef]

28. Tesfa, B.; Mishra, R.; Zhang, C.; Gu, F.; Ball, A.D. Combustion and performance characteristics of CI (compression ignition) engine running with biodiesel. *Energy* **2013**, *51*, 101–115. [CrossRef]

29. Das, M.; Sarkar, M.; Datta, A.; Santra, A.K. Study on viscosity and surface tension properties of biodiesel-diesel blends and their effects on spray parameters for CI engines. *Fuel* **2018**, *220*, 769–779. [CrossRef]

30. Roskilly, A.P.; Nanda, S.K.; Wang, Y.D.; Chirkowski, J. The performance and the gaseous emissions of two small marine craft diesel engines fuelled with biodiesel. *Appl. Therm. Eng.* **2008**, *28*, 872–880. [CrossRef]

31. Wu, F.; Wang, J.; Chen, W.; Shuai, S. A study on emission performance of a diesel engine fuelled with five typical methyl ester biodiesels. *Atmos. Environ.* **2009**, *43*, 1481–1485. [CrossRef]

32. Xue, J.L. Combustion characteristics, engine performances and emissions of waste edible oil biodiesel in diesel engine. *Renew. Sustain. Energy Rev.* **2013**, *23*, 350–365. [CrossRef]

33. Rinaldini, C.A.; Mattarelli, E.; Savioli, T.; Cantore, G.; Garbero, M.; Bologna, A. Performance, emission and combustion characteristics of IDI engine running on waste plastic oil. *Fuel* **2016**, *183*, 292–303. [CrossRef]

34. Baskovi, U.Z.; Vihar, R.; Seljak, T.; Katrasnik, T. Combustion and emission formation phenomena of tire pyrolysis oil in a common rail Diesel engine. *Energy Convers. Manag.* **2017**, *149*, 706–721.

35. Rajak, U.; Nashine, P.; Chaurasiya, P.K.; Verma, T.N.; Patel, D.K.; Dwivedi, G. Experimental & predicative analysis of engine characteristics of various biodiesels. *Fuel* **2021**, *285*, 119097.

36. Mirhashemi, F.S.; Sadrnia, H. NOx emissions of compression ignition engines fueled with various biodiesel blends: A review. *J. Energy Inst.* **2020**, *93*, 129–151. [CrossRef]